

Microscopic Optical Potentials from Coupled Cluster Calculations

J. Rotureau

In collaboration with:

P. Danielewicz

G. Hagen

F. Nunes

T. Papenbrock



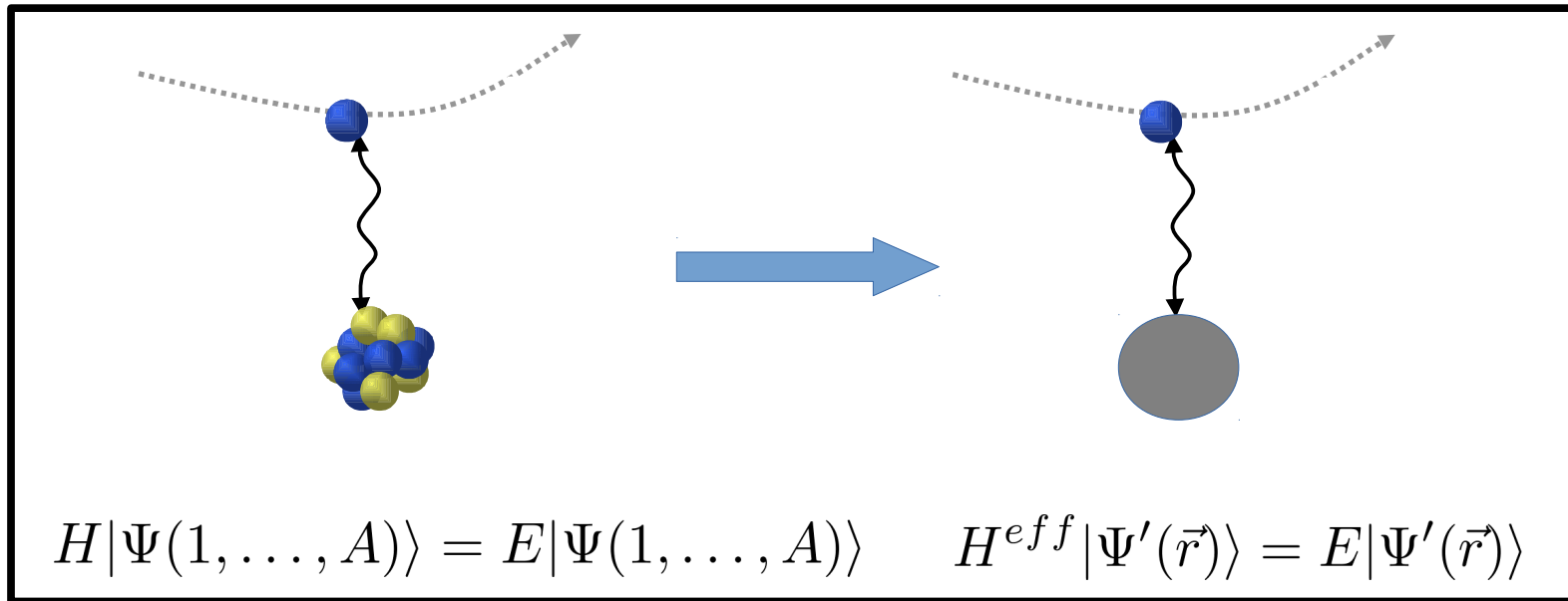
MICHIGAN STATE
UNIVERSITY



ICNT workshop, FRIB, East Lansing, July 2016.

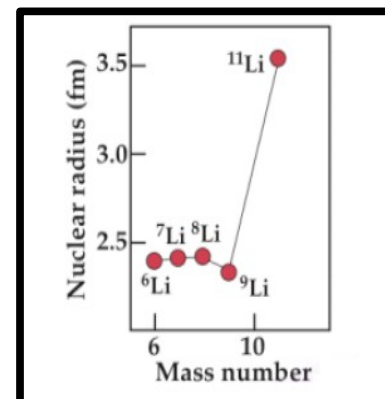
Goals

- * microscopic construction of optical potentials : nucleons as degrees of freedom, modern realistic n-n, 3n forces...

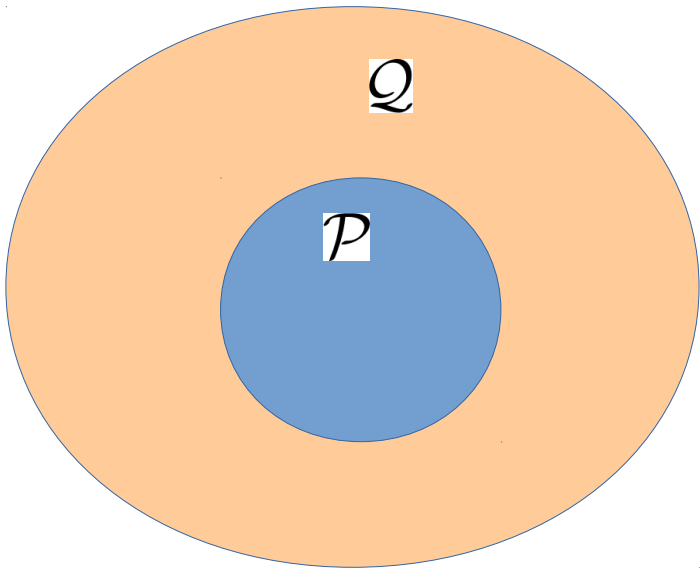


- * predictive theory for nuclear reactions

- * reliable/accurate extrapolations for systems far from stability.



Feshbach projection technique



$$\left\{ \begin{array}{l} |\Psi\rangle = |\Psi_P\rangle + |\Psi_Q\rangle \\ H = H_{PP} + H_{PQ} + H_{QP} + H_{QQ} \end{array} \right.$$

$$(E - H_{PP})|\Psi_P\rangle = H_{PQ}|\Psi_Q\rangle$$

$$(E - H_{QQ})|\Psi_Q\rangle = H_{QP}|\Psi_P\rangle$$

$$\left[E - \left(H_{PP} - H_{PQ} \frac{1}{E - H_{QQ}} H_{QP} \right) \right] |\Psi_P\rangle = 0$$



Effective (optical) potential:
→ energy-dependent, non local
→ complex (open quantum system)

Continuum Shell Model / Shell Model Embedded in the continuum:

H.W.Batz et al, NPA (1977) ; R.J. Philpott, NPA (1977) ;
K. Bennaceur et al, NPA(1999) ; J. Okołowicz, M. Płoszajczak,
I. Rotter, PR (2003) ; J. R et al, PRL (2005).

Single-particle Green's function

$$G(\alpha, \beta, E) = \langle \Psi_0^A | a_\alpha \frac{1}{E - (H - E_0^A) + i\eta} a_\beta^\dagger | \Psi_0^A \rangle \\ + \langle \Psi_0^A | a_\beta^\dagger \frac{1}{E + (E_0^A - H) - i\eta} a_\alpha | \Psi_0^A \rangle$$

$\eta \rightarrow 0$

Lehman representation

$$G(\alpha, \beta; E) = \sum_n \frac{\langle \Psi_0^A | a_\alpha | \Psi_n^{A+1} \rangle \langle \Psi_n^{A+1} | a_\beta^\dagger | \Psi_0^A \rangle}{E - [E_n^{A+1} - E_0^A] + i\eta} + \sum_m \frac{\langle \Psi_0^A | a_\beta^\dagger | \Psi_m^{A-1} \rangle \langle \Psi_m^{A-1} | a_\alpha | \Psi_0^A \rangle}{E - [E_0^A - E_m^{A-1}] - i\eta}$$

Connection to experimental data:

i) poles: energy of the $A+1$ and $A-1$ nuclei with respect to the g.s. of the A -nucleon system

ii) spectral functions :

$$E \leq \epsilon_F^- = E_0^A - E_0^{A-1}$$

$$S_h(\alpha; E) = \frac{1}{\pi} \text{Im } G(\alpha, \alpha; E) = \sum_m |\langle \Psi_m^{A-1} | a_\alpha | \Psi_0^A \rangle|^2 \delta(E - (E_0^A - E_m^{A-1}))$$

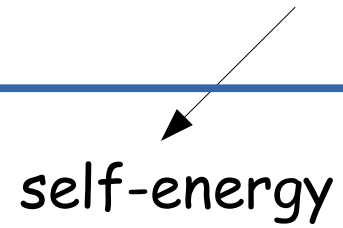
$$S_p(\alpha; E) = -\frac{1}{\pi} \text{Im } G(\alpha, \alpha; E) = \sum_n |\langle \Psi_n^{A+1} | a_\alpha^\dagger | \Psi_0^A \rangle|^2 \delta(E - (E_n^{A+1} - E_0^A))$$

$$E \geq \epsilon_F^+ = E_0^{A+1} - E_0^A$$

"measure" of the correlations in nuclei as their behaviors deviate from an independent particle model

Dyson equation

$$G(\alpha, \beta; E) = G^{(0)}(\alpha, \beta; E) + \sum_{\gamma, \delta} G^{(0)}(\alpha, \gamma; E) \Sigma(\gamma, \delta; E) G(\delta, \beta; E)$$



A diagram illustrating the Dyson equation. A horizontal blue rectangular box contains the equation $G(\alpha, \beta; E) = G^{(0)}(\alpha, \beta; E) + \sum_{\gamma, \delta} G^{(0)}(\alpha, \gamma; E) \Sigma(\gamma, \delta; E) G(\delta, \beta; E)$. An arrow points from the text "self-energy" below the box to the term $\Sigma(\gamma, \delta; E)$ in the equation.

self-energy

Dyson equation

$$G(\alpha, \beta; E) = G^{(0)}(\alpha, \beta; E) + \sum_{\gamma, \delta} G^{(0)}(\alpha, \gamma; E) \Sigma(\gamma, \delta; E) G(\delta, \beta; E)$$

self-energy

$$z_n^{A-1}(r) = \langle \Psi_n^{A-1} | a_r | \Psi_0^A \rangle$$

$$\xi_{E+}^c(r) = \langle \Psi_0^A | a_r | \Psi_{E+}^c \rangle$$

solutions of a one-body Schrödinger-like equation with the self-energy .

wave function for the elastic scattering from the g.s of the A -nucleon system

Our approach: calculation of the Green's function with the Coupled Cluster method.

$$G(\alpha, \beta, E) = \langle \Psi_0^A | a_\alpha \frac{1}{E - (H - E_0^A) + i\eta} a_\beta^\dagger | \Psi_0^A \rangle \\ + \langle \Psi_0^A | a_\beta^\dagger \frac{1}{E + (E_0^A - H) - i\eta} a_\alpha | \Psi_0^A \rangle$$

Previous applications in Quantum Chemistry:

M. Nooijen, J. G. Snijders; J. Quantum Chem. 44 (1992) 55,...,
Kowalski K, K Bhaskaran-Nair, and WA Shelton; J. Chem. Phys. 141
(2014) 094102.

Coupled cluster

Exponential ansatz for the many-body wave function :

$$|\Psi\rangle = e^T |\Phi\rangle$$

G. Hagen, T. Papenbrock, M. Hjorth-Jensen,
D. J. Dean, Rep. Prog. Phys. (2014)

1p-1h operator

$$T = T_1 + T_2 + \dots$$

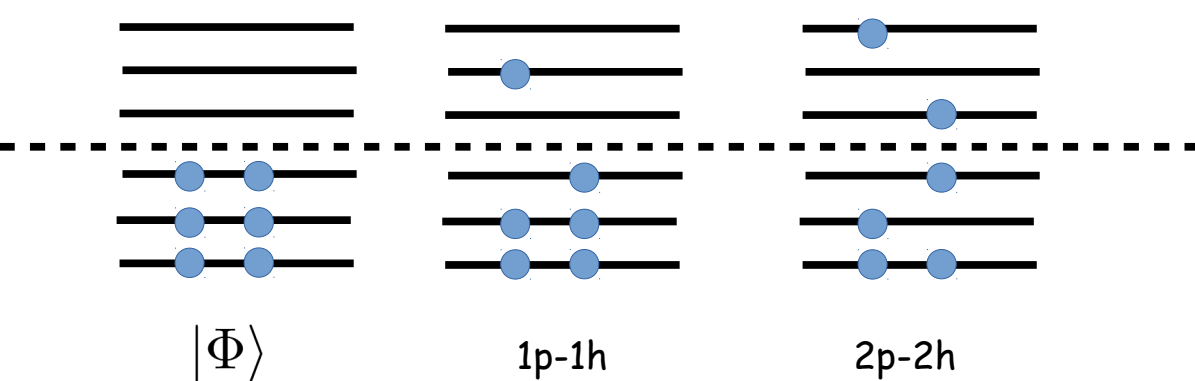
2p-2h operator

Similarity-transformed Hamiltonian

$$\bar{H} = e^{-T} H e^T$$

Coupled-cluster equations

$$\begin{aligned} E &= \langle \Phi | \bar{H} | \Phi \rangle \\ 0 &= \langle \Phi_i^a | \bar{H} | \Phi \rangle \\ 0 &= \langle \Phi_{ij}^{ab} | \bar{H} | \Phi \rangle \\ &\dots \end{aligned}$$



Elastic proton scattering of medium mass nuclei from coupled-cluster theory

G. Hagen^{1,2} and N. Michel²

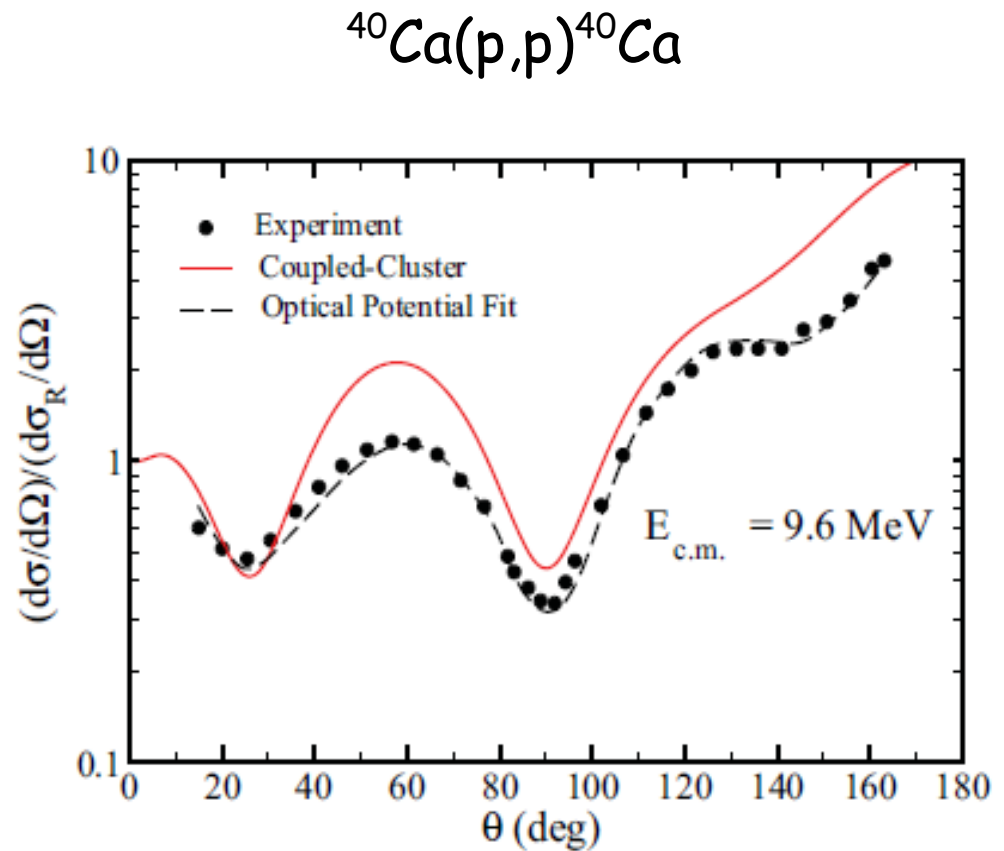
¹*Physics Division, Oak Ridge National Laboratory, Oak Ridge, Tennessee 37831, USA*

²*Department of Physics and Astronomy, University of Tennessee, Knoxville, Tennessee 37996, USA*

(Received 11 June 2012; revised manuscript received 24 July 2012; published 13 August 2012)

One-nucleon overlap function

$$O_A^{A+1}(lj; kr) = \sum_n \langle A + 1 | |\tilde{a}_{nlj}^\dagger| |A \rangle \phi_{nlj}(r)$$



NN interaction: N²LO_{opt}

PRL 110, 192502 (2013)

PHYSICAL REVIEW LETTERS

week ending
10 MAY 2013

Optimized Chiral Nucleon-Nucleon Interaction at Next-to-Next-to-Leading Order

A. Ekström,^{1,2} G. Baardsen,¹ C. Forssén,³ G. Hagen,^{4,5} M. Hjorth-Jensen,^{1,2,6} G. R. Jansen,^{4,5} R. Machleidt,⁷ W. Nazarewicz,^{5,4,8} T. Papenbrock,^{5,4} J. Sarich,⁹ and S.M. Wild⁹

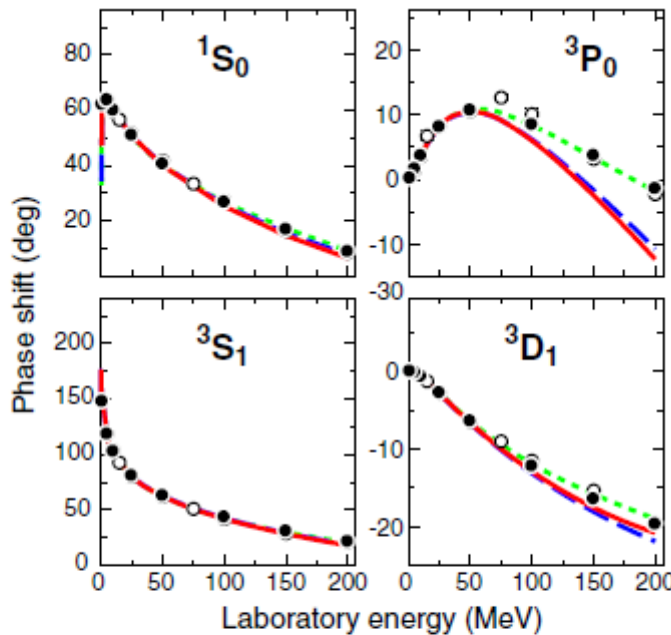
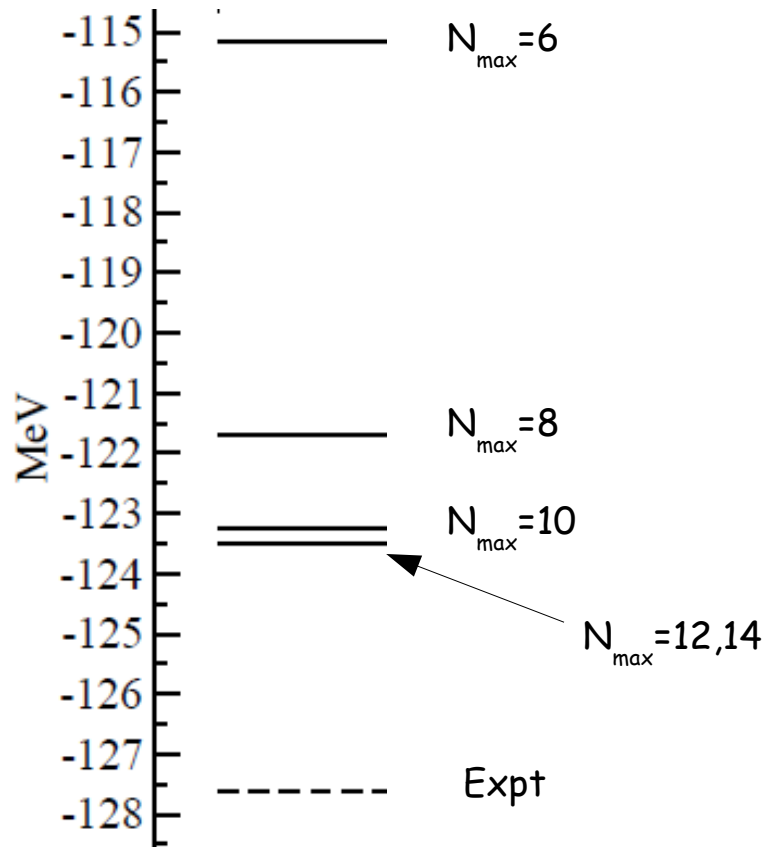


FIG. 1 (color online). Computed np phase shifts of the optimized NNLO potential of this work (solid, red line), the NNLO potential of Ref. [3] (dashed, blue line), and the N³LO potential [4] (green, dotted line) compared with the Nijmegen phase shift analysis [18] (solid dots) and the VPI/GWU analysis SM99 [43] (open circles).

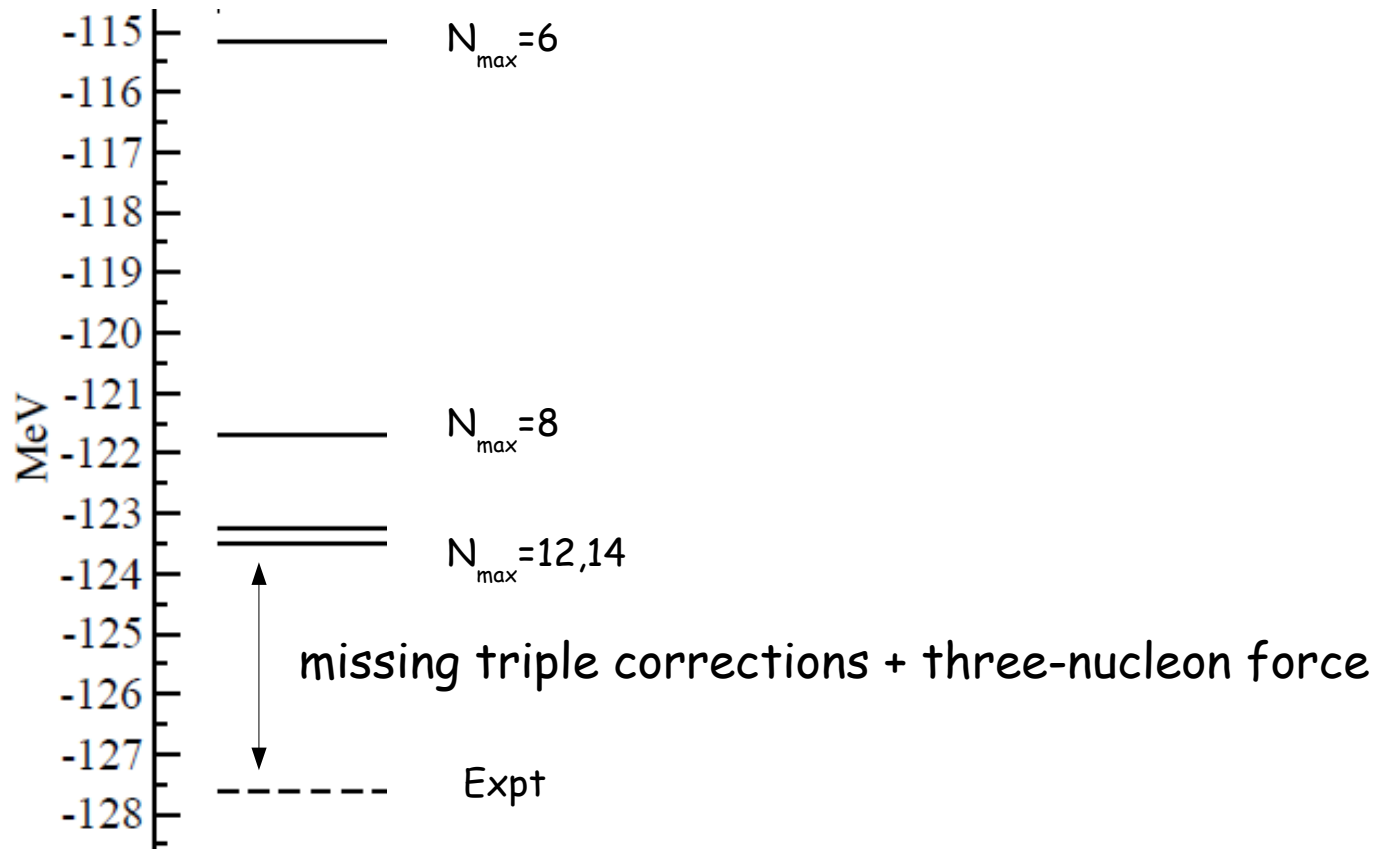
Coupled Cluster (SD) for ^{16}O and ^{17}O with $\text{N}^2\text{LO}_{\text{opt}}$

^{16}O ground state



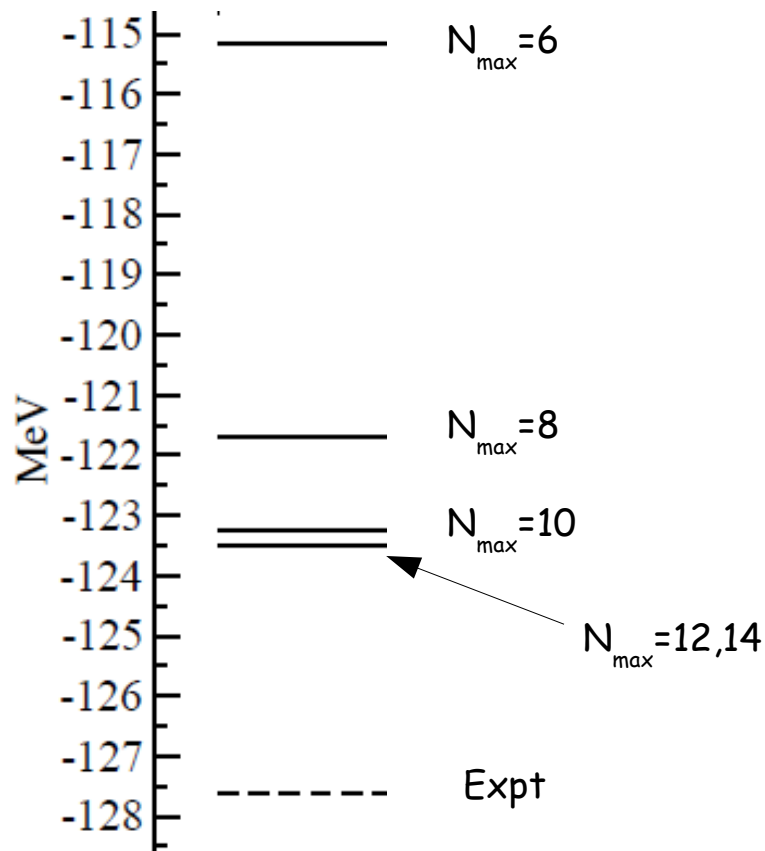
Coupled Cluster (SD) for ^{16}O and ^{17}O with $\text{N}^2\text{LO}_{\text{opt}}$

^{16}O ground state

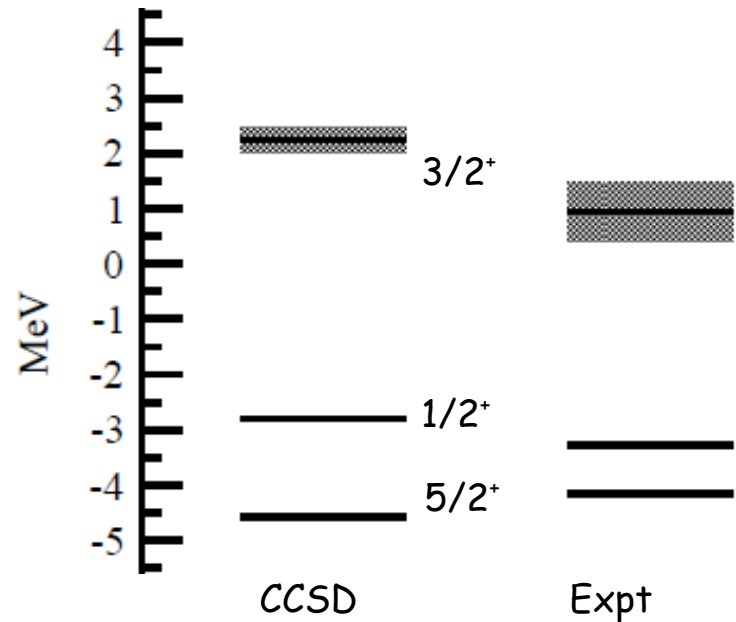


Coupled Cluster (SD) for ^{16}O and ^{17}O with $\text{N}^2\text{LO}_{\text{opt}}$

^{16}O ground state



^{17}O



Coupled Cluster Green's function

$$\begin{aligned} G(\alpha, \beta; E) &= \langle \Phi_L | \bar{a}_\alpha \frac{1}{E - [\bar{H} - E_0^A] + i\eta} \bar{a}_\beta^\dagger | \Phi \rangle \\ &+ \langle \Phi_L | \bar{a}_\beta^\dagger \frac{1}{E - [E_0^A - \bar{H}] - i\eta} \bar{a}_\alpha | \Phi \rangle \end{aligned}$$

→ similarity-transformed operators :

$$\bar{a}_\alpha^\dagger = e^{-T} a_\alpha^\dagger e^T$$

$$\bar{a}_\alpha = e^{-T} a_\alpha e^T$$

→ Inversion of the (similarity-transformed) Hamiltonian in the Lanczos basis :

$$\{\langle \Phi_L | \bar{a}_\alpha, \langle \Phi_L | \bar{a}_\alpha \bar{H}, \langle \Phi_L | \bar{a}_\alpha \bar{H}^2, \dots, \bar{H}^2 \bar{a}_\beta^\dagger | \Phi \rangle, \bar{H} \bar{a}_\beta^\dagger | \Phi \rangle, a_\beta^\dagger | \Phi \rangle\}$$

Particle spectral function in ^{17}O

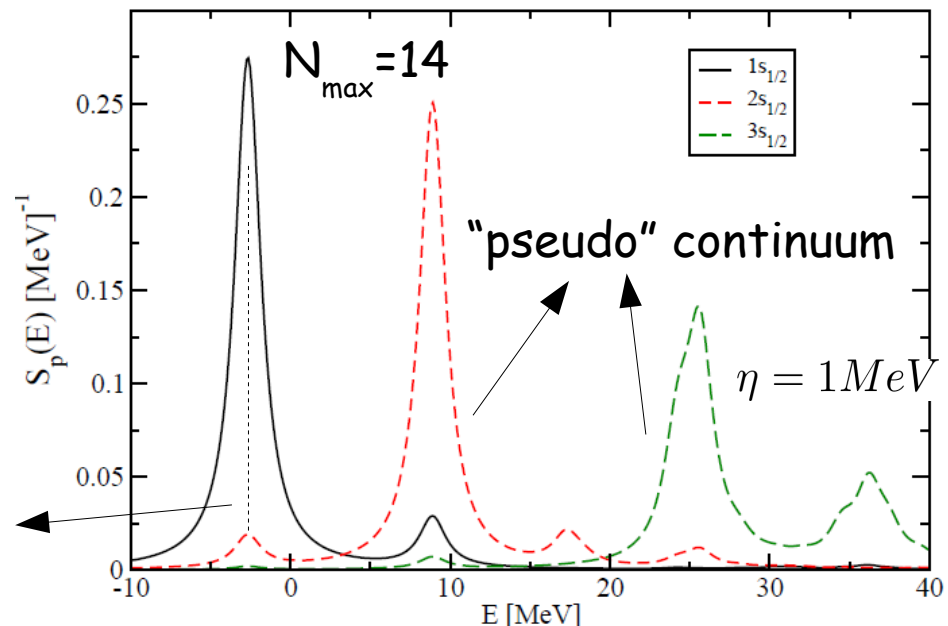
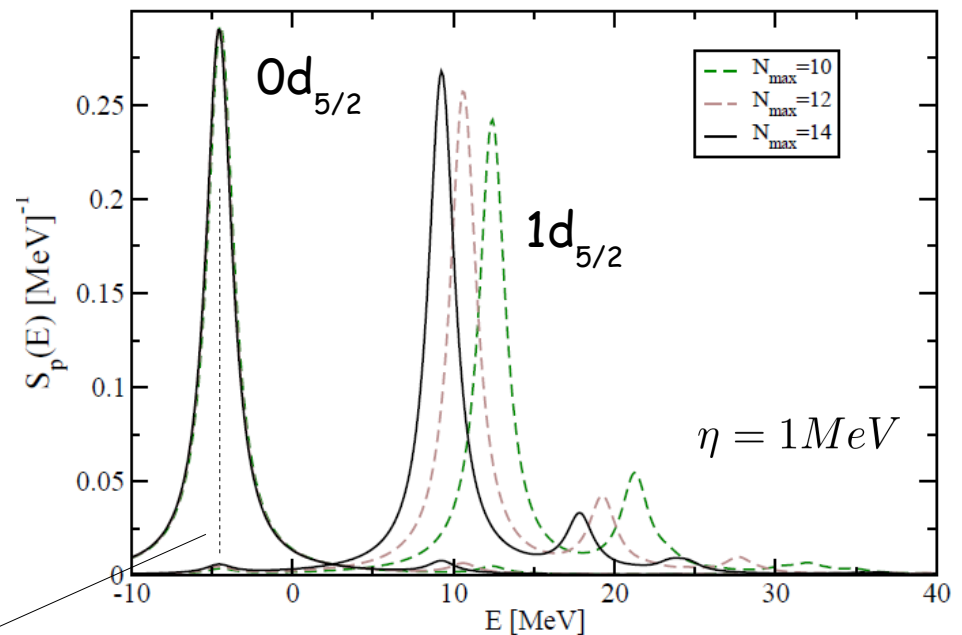
$$S_p(\alpha; E) = -\frac{1}{\pi} \text{Im } G(\alpha, \alpha; E)$$

CCSD (Single-Double):
 -> H.O. basis with $\hbar\omega=20$ MeV.

$$\begin{aligned} E^{\text{exp}}(5/2^+) &= -4.142 \text{ MeV} \\ E^{\text{exp}}(1/2^+) &= -3.272 \text{ MeV} \end{aligned}$$

1st excited state
 $E^{\text{ccsd}}(1/2^+) = -2.670 \text{ MeV}$

ground state
 $E^{\text{ccsd}}(5/2^+) = -4.557 \text{ MeV}$

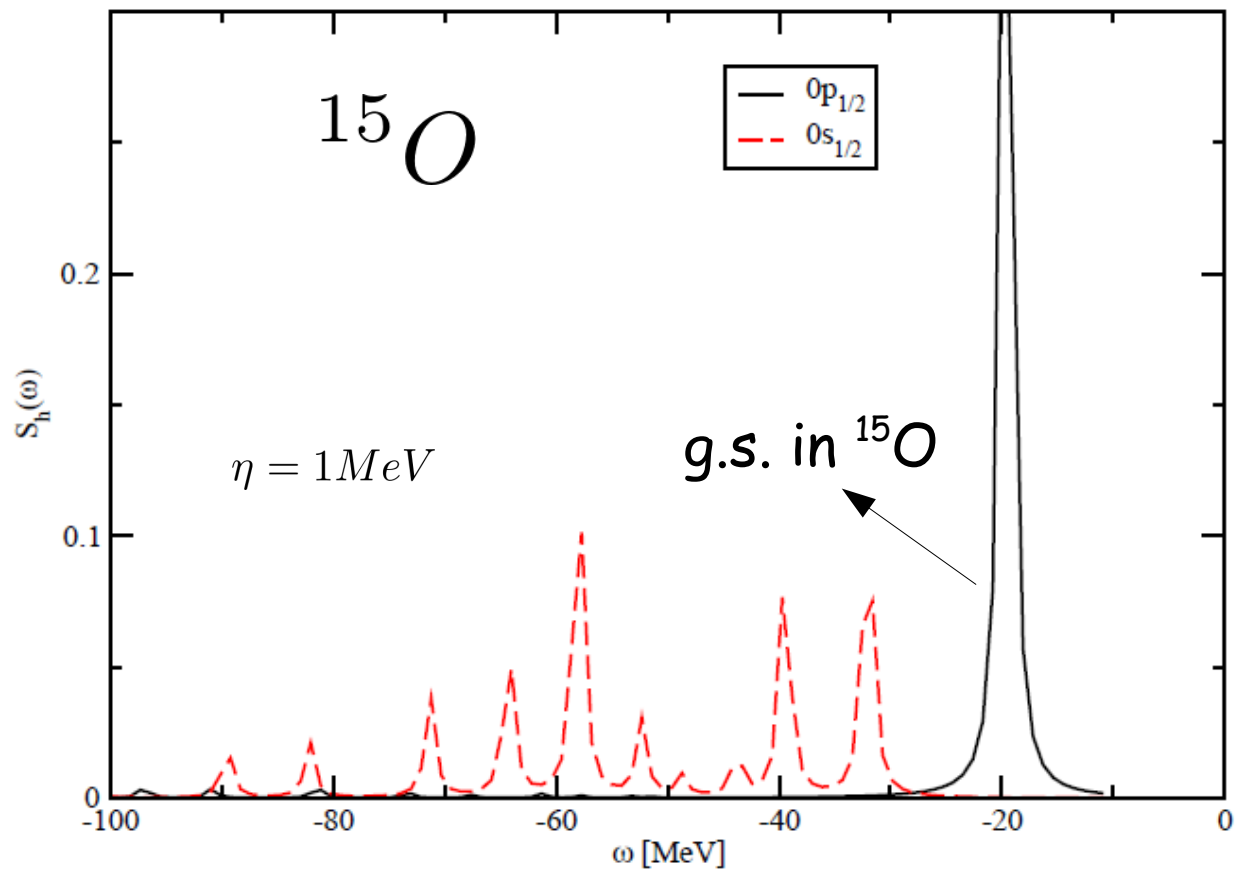


Hole spectral function in ^{15}O

CCSD (Single-Double):

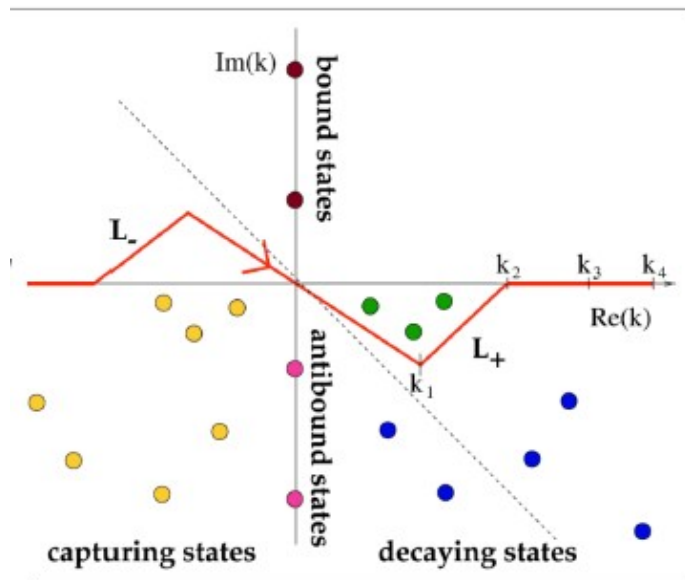
-> H.O. basis with $\hbar\omega=20$ MeV

-> $N_{\max}=14$



Green's function in the Berggren Basis

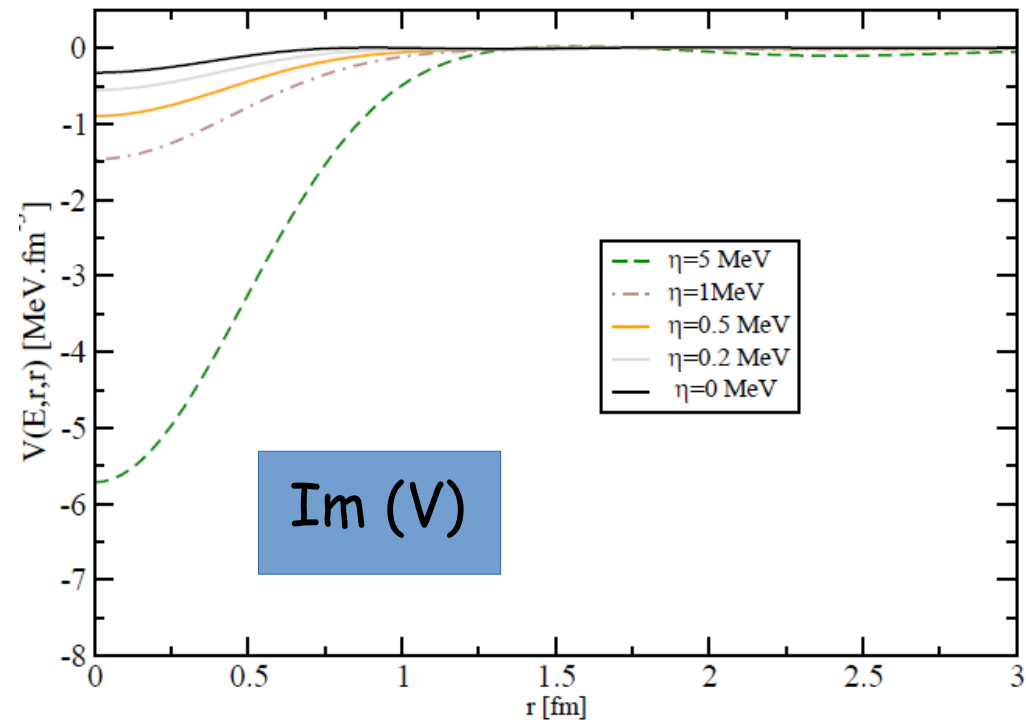
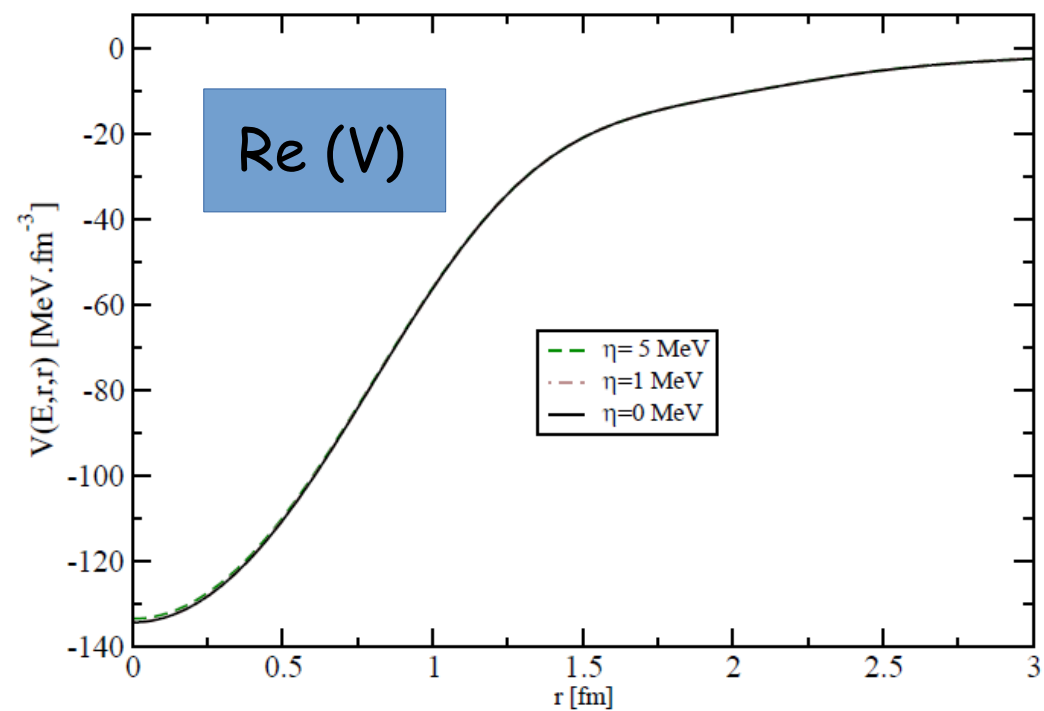
$$G(\alpha, \beta; E) = \sum_n \frac{\langle \Psi_0^A | a_\alpha | \Psi_n^{A+1} \rangle \langle \Psi_n^{A+1} | a_\beta^\dagger | \Psi_0^A \rangle}{E - [\tilde{E}_n^{A+1} - E_0^A] + i\eta} + \sum_m \frac{\langle \Psi_0^A | a_\beta^\dagger | \Psi_m^{A-1} \rangle \langle \Psi_m^{A-1} | a_\alpha | \Psi_0^A \rangle}{E - [E_0^A - \tilde{E}_m^{A-1}] - i\eta}$$



→ with the complex-continuum
the (numerical) Green's function
behaves smoothly as η goes to 0.

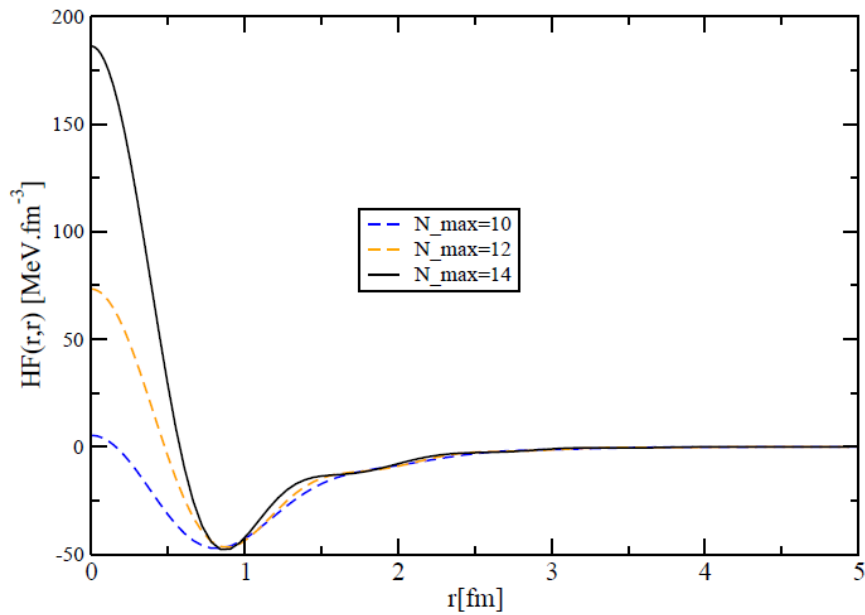
Berggren basis (T. Berggren, NPA 109 (1968))

Optical Potential for S-wave neutron elastic scattering at 10 MeV

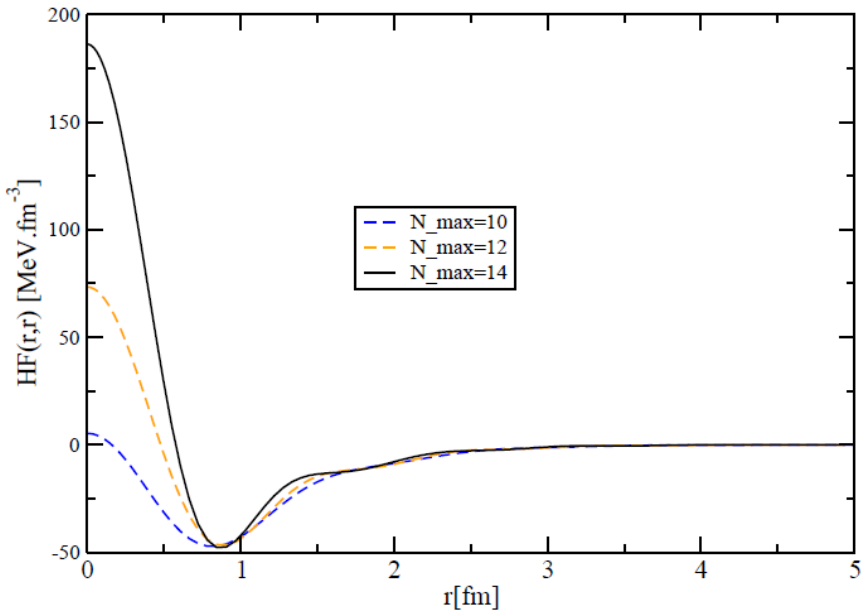


Mixed basis: H.O. shells ($N_{\max} = 10$) + 40 s-wave complex continuum

Convergence of the Hartree-Fock potential

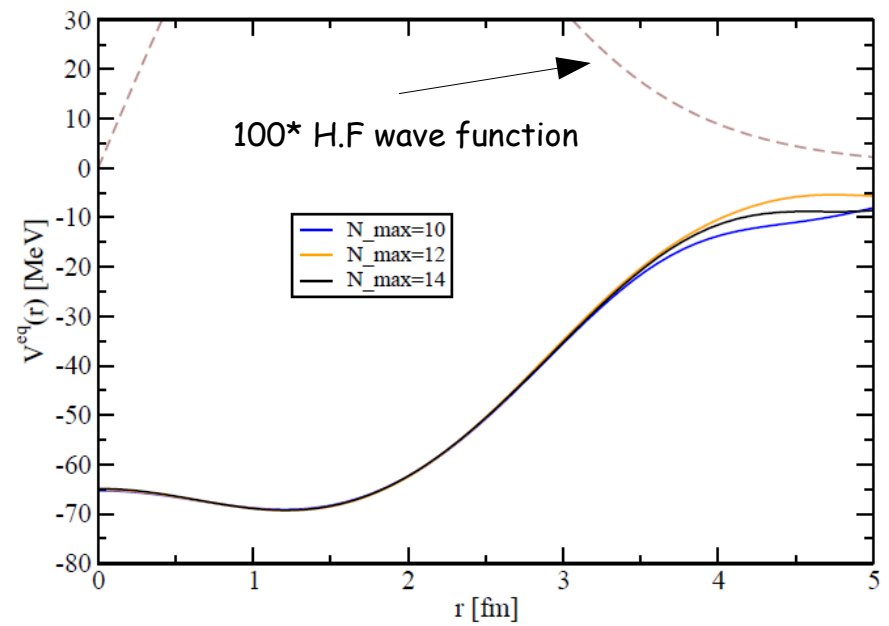


Convergence of the Hartree-Fock potential

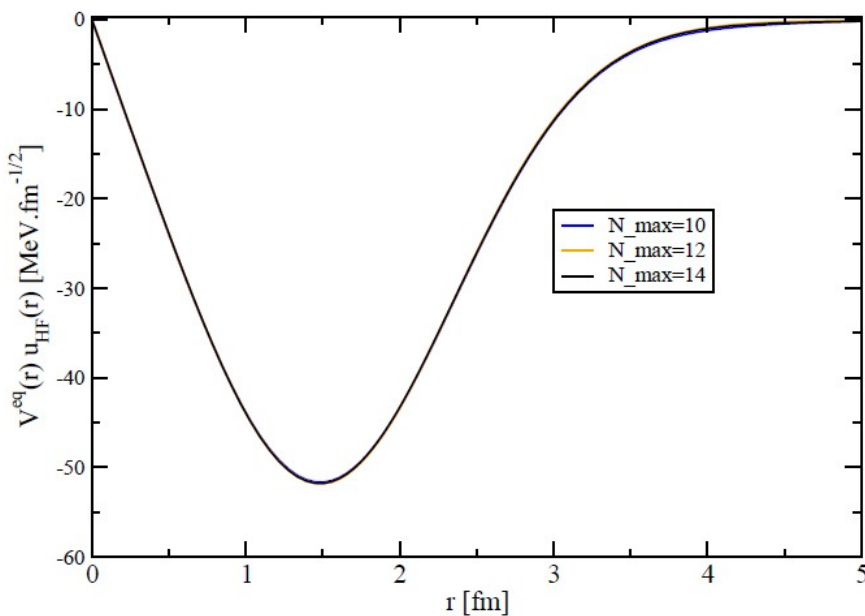
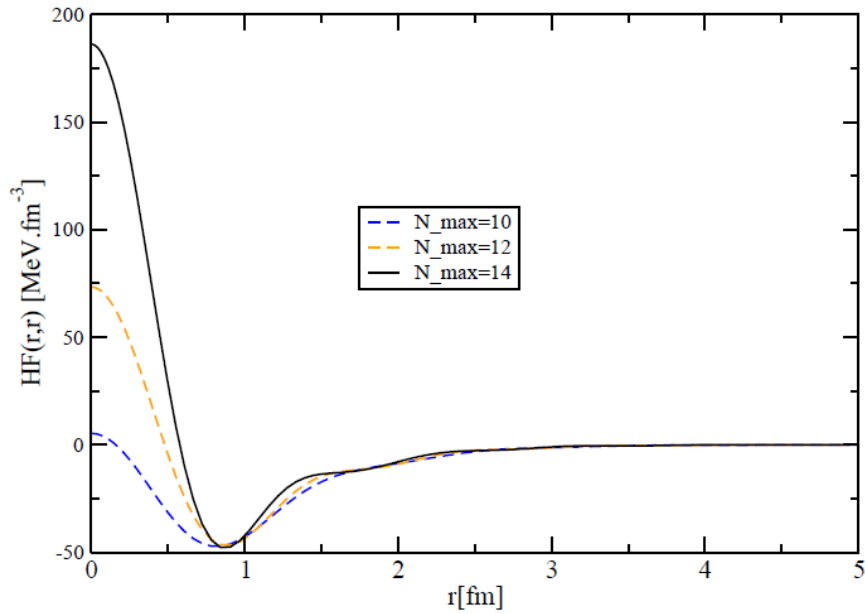


Equivalent Potential

$$V^{eq}(r) = r \int \frac{r' dr' V^{HF}(r, r') u_{HF}(r')}{u_{HF}(r)}$$

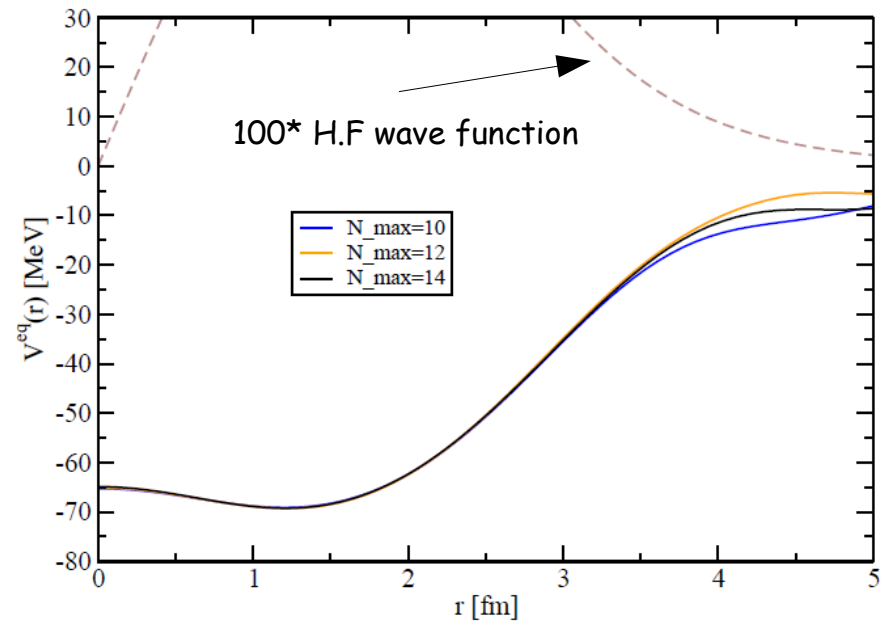


Convergence of the Hartree-Fock potential



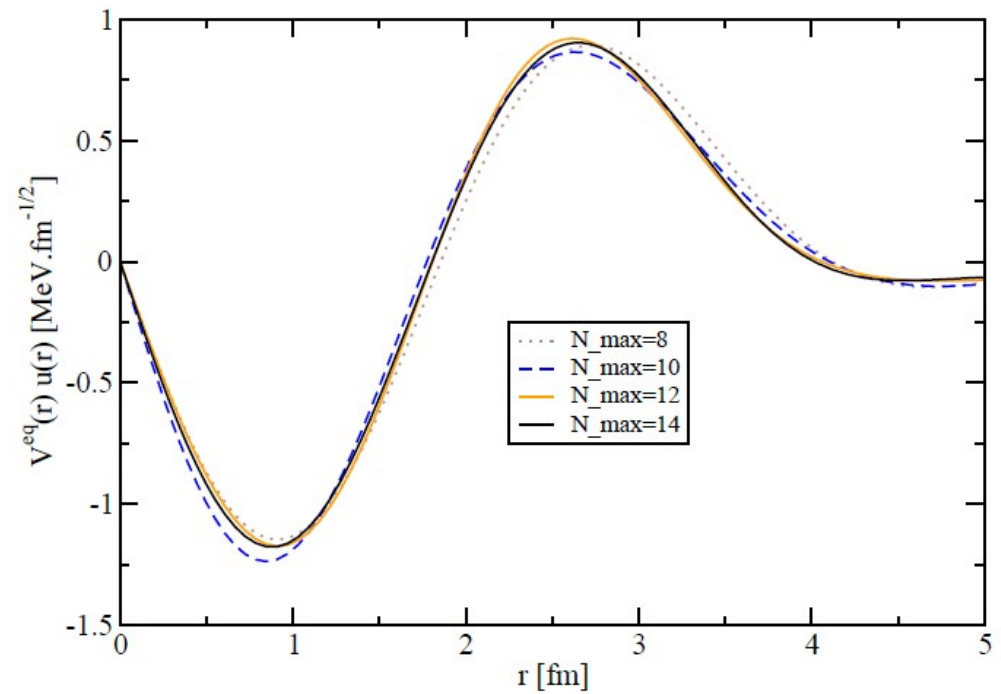
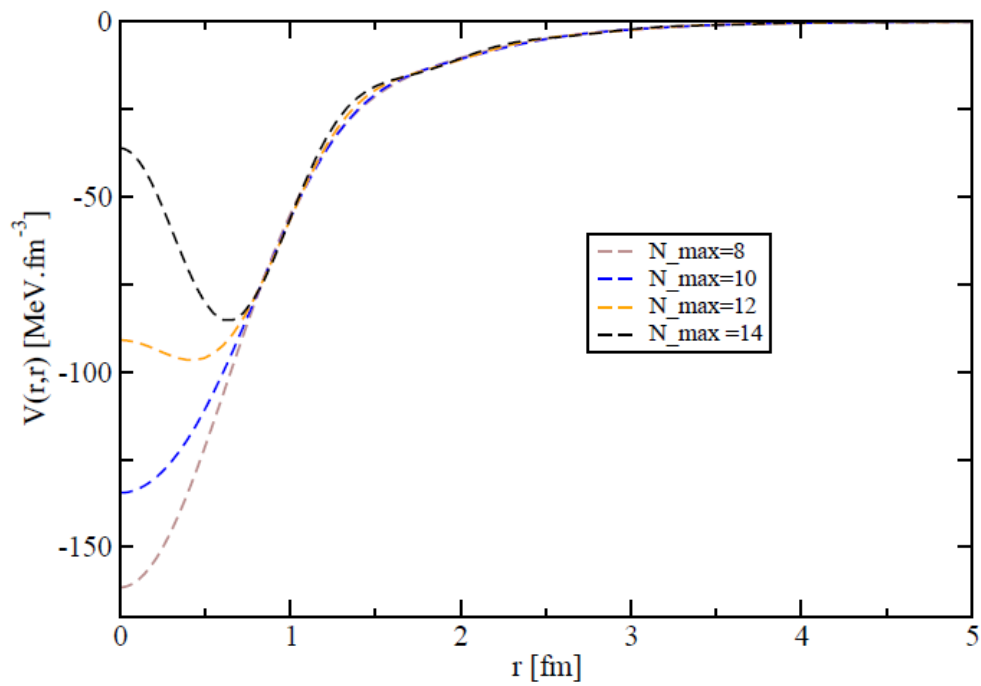
Equivalent Potential

$$V^{eq}(r) = r \int \frac{r' dr' V^{HF}(r, r') u_{HF}(r')}{u_{HF}(r)}$$



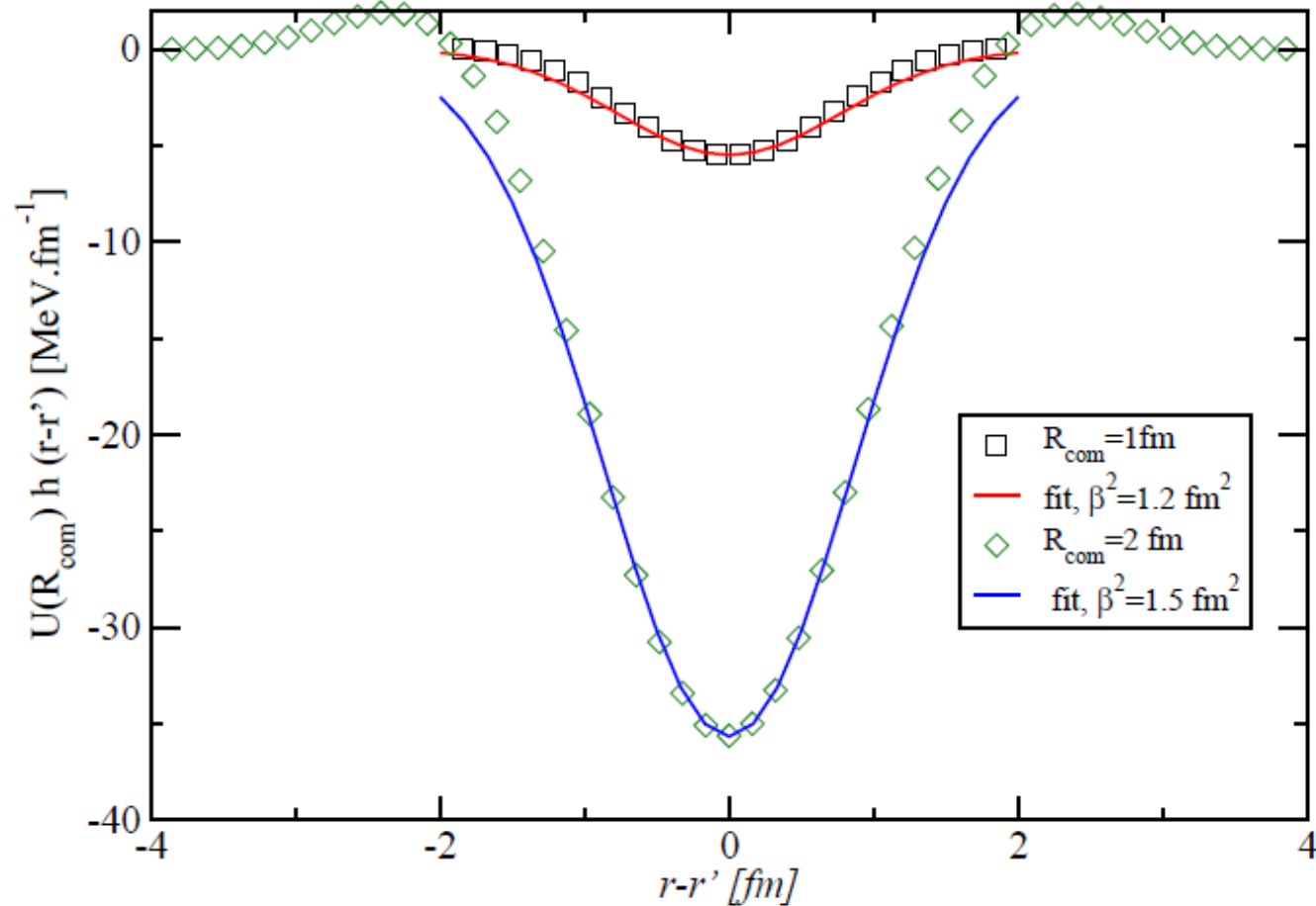
Convergence of the optical potential

S-wave neutron potential at 10 MeV



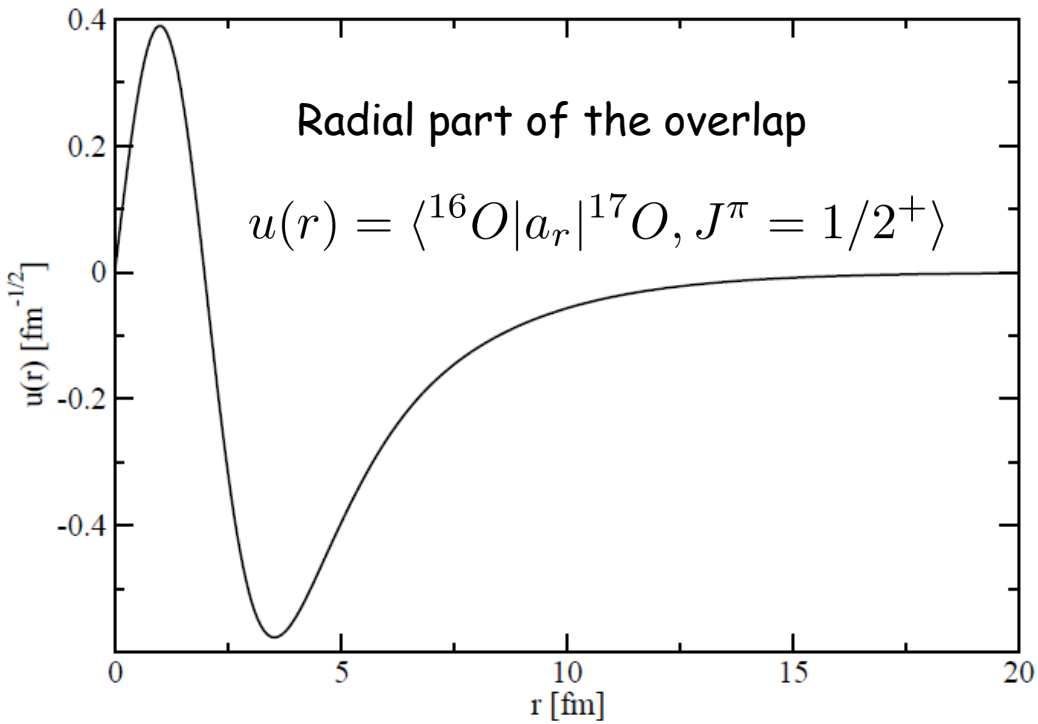
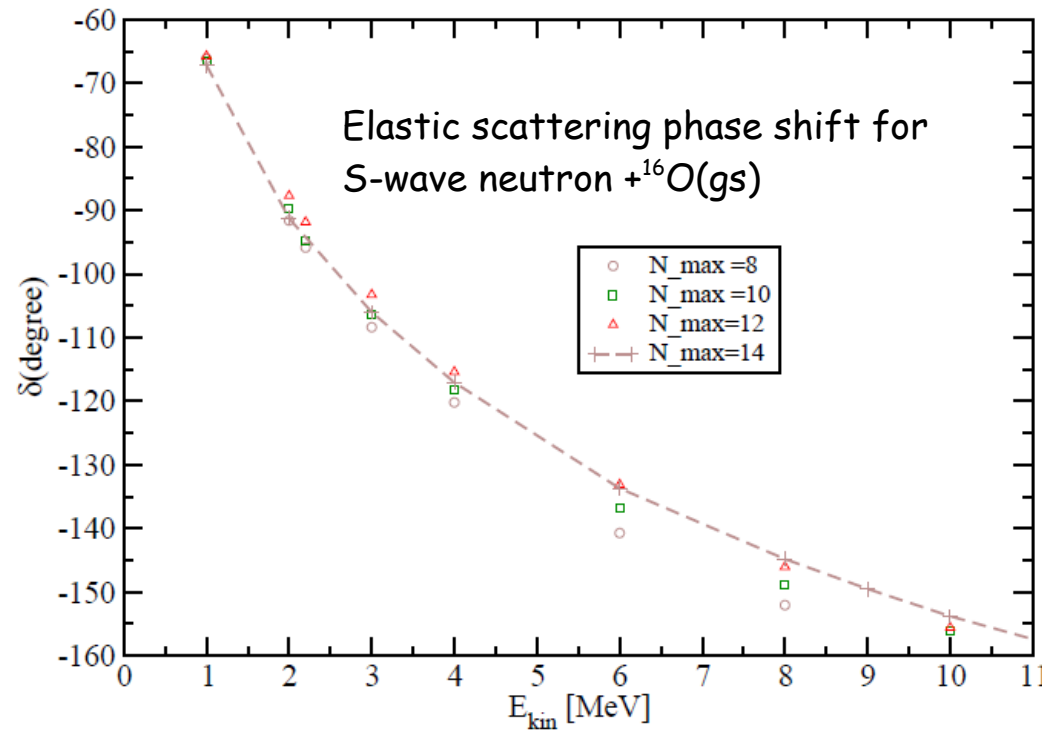
"Picture" of the non-locality

$$V(r, r') \equiv \frac{U(\frac{r+r'}{2})h(r - r')}{rr'}$$



$d_{5/2}$ -wave neutron potential at 1 MeV

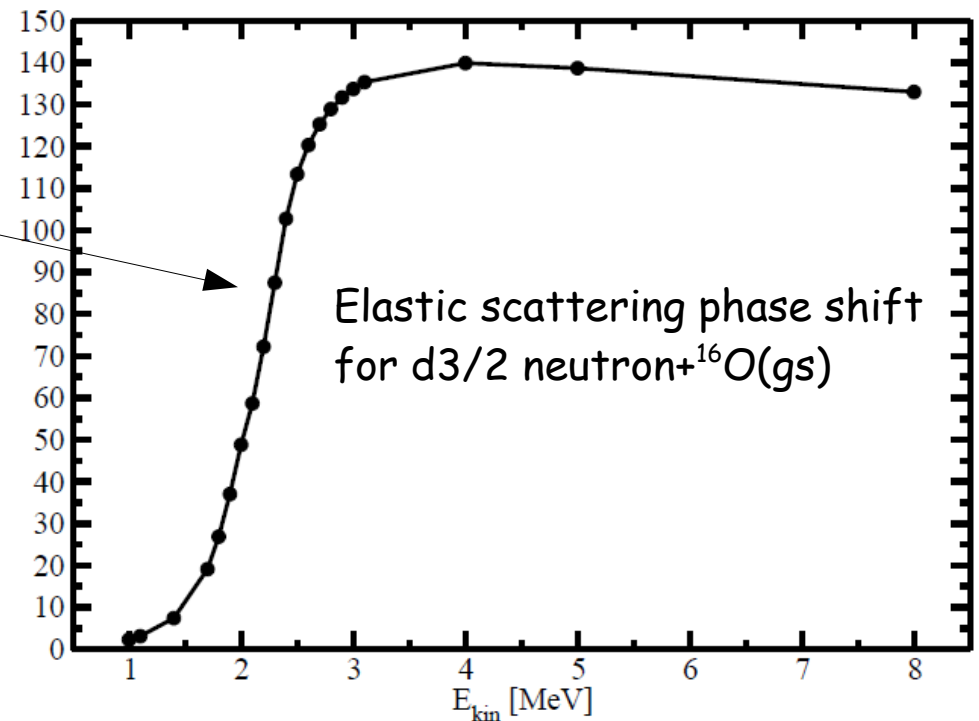
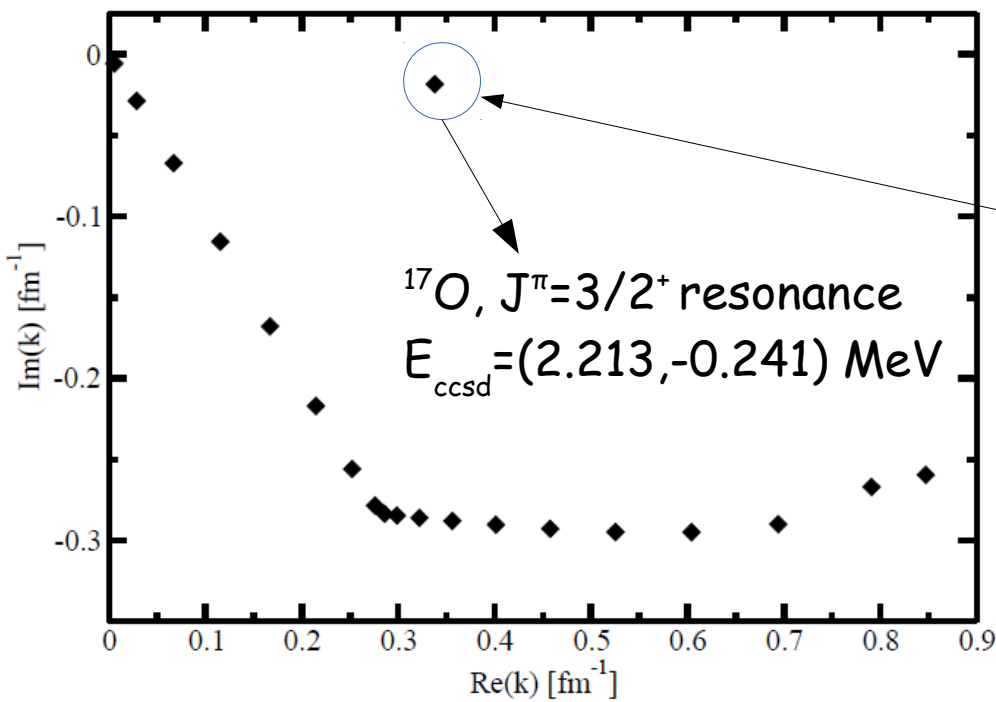
S-wave neutron



Mixed basis: H.O. shells +40 s-wave complex continuum shells

$d_{3/2}$ neutron

CCSD spectrum in k-space for $J^\pi=3/2^+$



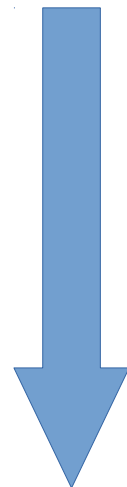
$$E^{\text{exp}}(3/2^+) = (0.943, -0.48) \text{ MeV}$$

Mixed basis:H.O. shells ($N_{\text{max}}=10$) + 40 $d_{3/2}$ -wave complex continuum

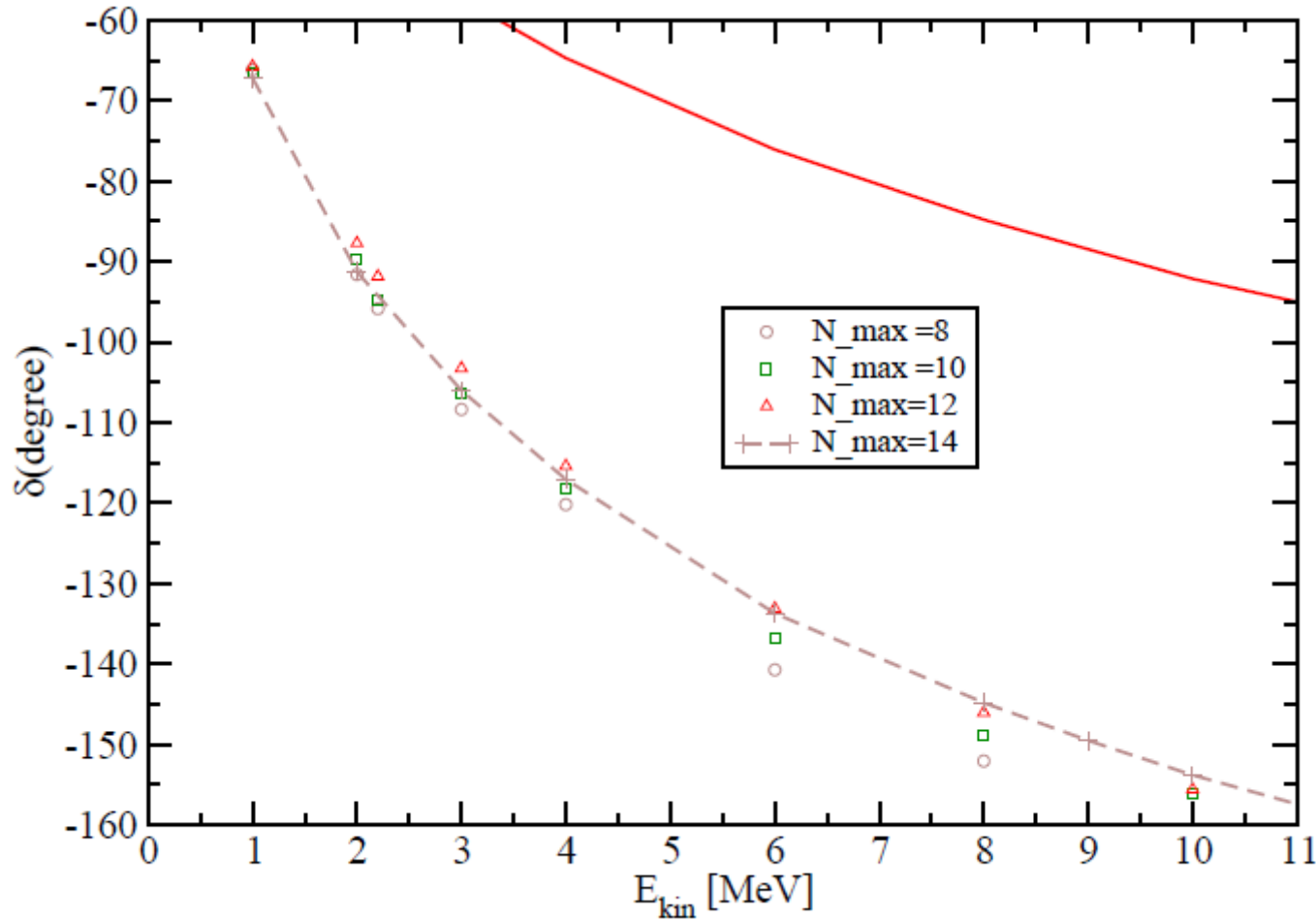
Towards Optical Potentials from Coupled Cluster Calculations

Combining the Many-body Green's function
and the Coupled-Cluster method.

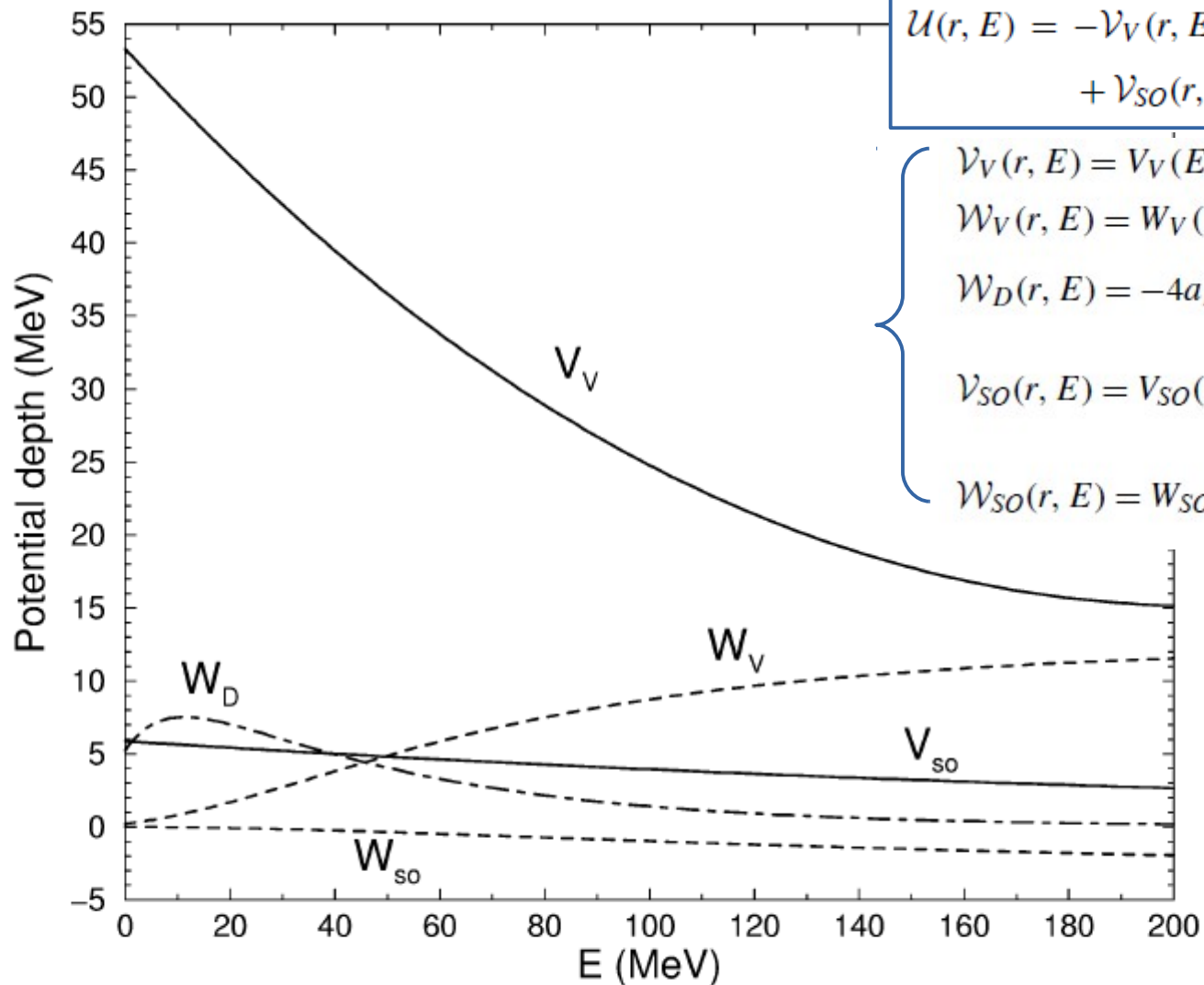
Ab-initio approach with n-n,
3n forces and coupling to the
continuum



Microscopic construction of optical potentials



Phenomenological Optical Potential



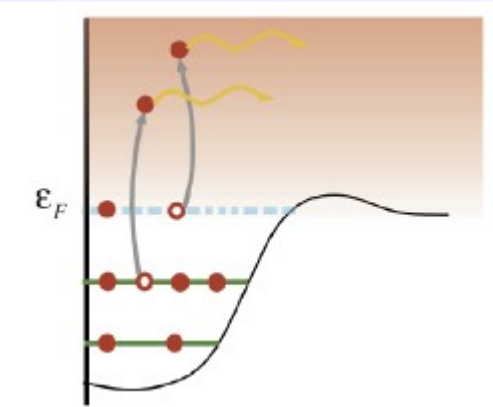
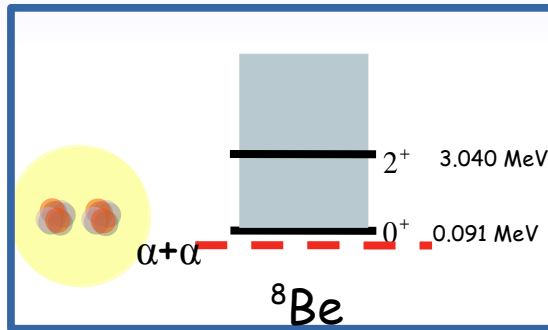
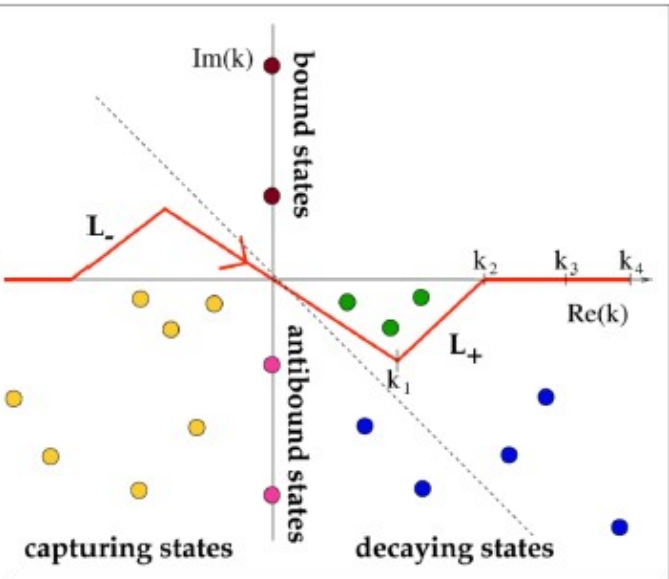
$$\begin{aligned} \mathcal{U}(r, E) = & -\mathcal{V}_V(r, E) - i\mathcal{W}_V(r, E) - i\mathcal{W}_D(r, E) \\ & + \mathcal{V}_{SO}(r, E)\mathbf{l}\cdot\boldsymbol{\sigma} + i\mathcal{W}_{SO}(r, E)\mathbf{l}\cdot\boldsymbol{\sigma} + \mathcal{V}_C(r), \end{aligned}$$

$$\left. \begin{aligned} \mathcal{V}_V(r, E) &= V_V(E)f(r, R_V, a_V), \\ \mathcal{W}_V(r, E) &= W_V(E)f(r, R_V, a_V), \\ \mathcal{W}_D(r, E) &= -4a_D W_D(E) \frac{d}{dr} f(r, R_D, a_D), \\ \mathcal{V}_{SO}(r, E) &= V_{SO}(E) \left(\frac{\hbar}{m_\pi c} \right)^2 \frac{1}{r} \frac{d}{dr} f(r, R_{SO}, a_{SO}), \\ \mathcal{W}_{SO}(r, E) &= W_{SO}(E) \left(\frac{\hbar}{m_\pi c} \right)^2 \frac{1}{r} \frac{d}{dr} f(r, R_{SO}, a_{SO}). \end{aligned} \right\}$$

Fig. 1. The various potential well depths as a function of incident (laboratory) energy, see Eq. (7). As an example, the values for neutrons incident on ^{56}Fe are plotted.

Berggren basis

Physics of nuclei at the edges of stability



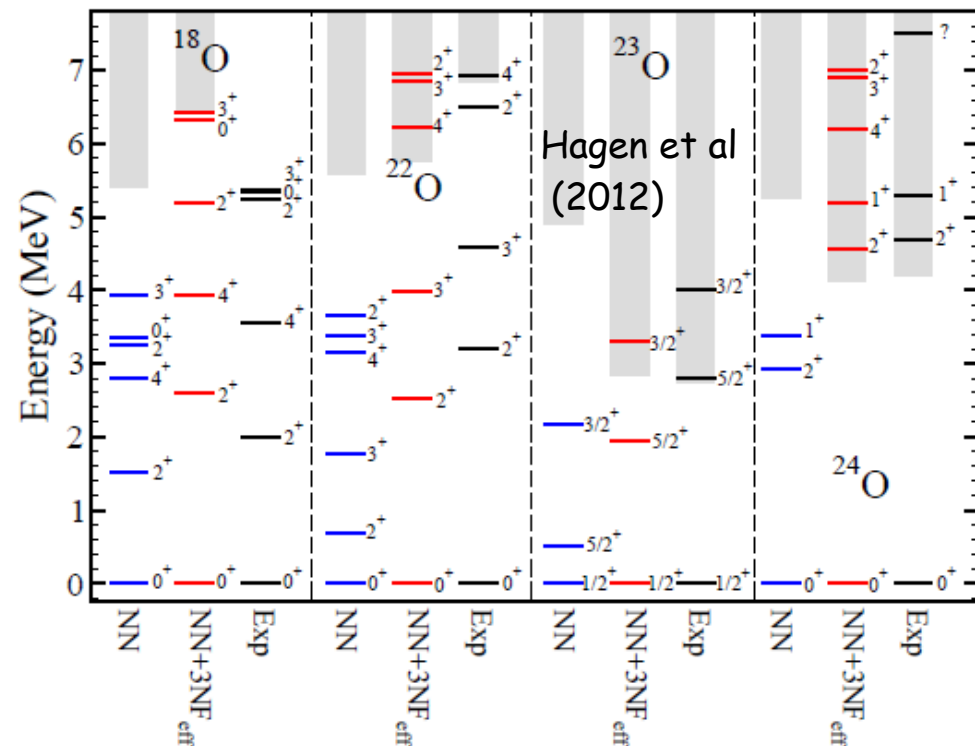
*coupling to the continuum is an essential feature of systems far from stability.
 *taken into account by using the Berggren basis which includes bound, resonant and scattering states.

Gamow (complex-energy) Shell Model :

N. Michel et al, PRL (2002); G. Hagen et al, PRC (2005);
 J.R et al, PRL (2006); N. Michel et al, JPG (2009); G.
 Papadimitriou et al, PRC (2014); Y. Jaganathan et al, JP
 (2012); K. Fossez et al, PRA (2015).

Coupled Cluster in the Gamow Basis:

G. Hagen et al; PLB (2007), PRC (2009), PRL (2010), PRL
 (2012), RPP (2014).



Convergence pattern with the number of Lanczos iterations

